第 33 卷第 2 期
2017 年 2 月

无 机 化 学 学 报
CHINESE JOURNAL OF INORGANIC CHEMISTRY

Vol.33 No.2
227-236

由半刚性三羧酸配体构筑的一维和二维钴(Ⅱ)配位聚合物的合成、晶体结构及磁性质

顾文君[1] 顾金忠*,[2]

([1]西南大学动物科技学院,重庆 400715)

([2]兰州大学化学化工学院,兰州 730000)

摘要:采用水热方法,用半刚性三羧酸配体(H_3cpta)和菲咯啉(phen)或 2,2′-联吡啶(2,2′-bipy)与 $CoCl_2·6H_2O$ 反应,合成了一个一维链状配位聚合物[Co(μ_2-Hcpta)(phen)(H_2O)]$_n$(**1**)和一个二维层状配位聚合物[Co_3(μ_5-cpta)$_2$(2,2′-bipy)$_2$]$_n$(**2**),并对其结构和磁性质进行了研究。结构分析结果表明 2 个配合物均属于单斜晶系,$P2_1/c$ 空间群。配合物 **1** 具有一维链状结构,而且这些一维链状结构通过 C-H…O 氢键作用进一步形成了二维超分子网络。而配合物 **2** 具有由三核钴单元构筑的二维层状结构。研究表明,配合物 **1** 和 **2** 中相邻钴离子间存在反铁磁相互作用。

关键词:配位聚合物;氢键;三羧酸配体;磁性

中图分类号:O614.81+2 **文献标识码**:A **文章编号**:1001-4861(2017)02-0227-10

DOI:10.11862/CJIC.2017.035

Syntheses, Crystal Structures and Magnetic Properties of 1D and 2D Cobalt (Ⅱ) Coordination Polymers Constructed from Semir-igid Tricarboxylic Acid

GU Wen-Jun[1] GU Jin-Zhong*,[2]

([1]*College of Animal Science and Technology, Southwest University, Chongqing* 400715, *China*)

([2]*College of Chemistry and Chemical Engineering, Lanzhou University, Lanzhou* 730000, *China*)

Abstract: Two 1D and 2D cobalt(Ⅱ) coordination polymers, namely [Co(μ_2-Hcpta)(phen)(H_2O)]$_n$ (**1**) and [Co_3(μ_5-cpta)$_2$(2,2′-bipy)$_2$]$_n$(**2**), have been constructed hydrothermally using H_3cpta (H_3cpta=2-(2-carboxyphenoxy)terephthalic acid), phen (phen=phenanthroline) or 2,2′-bipy (2,2′-bipy=2,2′-bipyridine), and cobalt chloride. Single-crystal X-ray diffraction analyses revealed that the two compounds crystallize in the monoclinic system, space group $P2_1/c$. In compound **1**, the carboxylate groups of $Hcpta^{2-}$ ligands bridge alternately neighboring metal ions to form a chain. Adjacent chains are assembled to a 2D supramolecular network through C-H…O hydrogen bond. Compound **2** shows a 2D sheet based on Co_3 units. Magnetic studies for compounds **1** and **2** demonstrate an antiferromagnetic coupling between the adjacent Co(Ⅱ) centers. CCDC: 1507502, **1**; 1507503, **2**.

Keywords: coordination polymer; hydrogen bonding; tricarboxylic acid; magnetic properties

0 Introduction

The design and construction of the coordination polymers has attracted great attention for their potential applications, architectures, and topologies[1-8]. Many factors such as the coordination geometry of the central atom, the structural characteristics of the ligand, the solvent system, and the counterions can

收稿日期:2016-09-30。收修改稿日期:2016-12-02。

*通信联系人。E-mail:gujzh@lzu.edu.cn;会员登记号:S06N5892M1004。

play the key role in the construction of the coordination networks[9-12]. The selection of the special ligands is very important in the construction of these coordination polymers.

A lot of aromatic polycarboxylic acids has been extensively applied as multifunctional building blocks in the construction of metal-organic networks because of their abundant coordination modes to metal ions, allowing different type of structural topologies and because of their ability to act as H-bond acceptors and donors, depending on the number of deprotonated carboxylic groups to assemble supramolecular structures [13-16]. Among them, semi-rigid V-shaped ligands enable the formation of uncommon frameworks or even novel topologies and interesting properties because of their flexibility and conformational diversity[17-20].

In order to extend our research in this field, we chose a new semi-rigid polycarboxylate ligand, 2-(2-carboxyphenoxy)terephthalic acid (H_3cpta) to construct novel coordination polymers. The H_3cpta ligand possesses the following features: (1) two rigid benzene rings of H_3cpta ligand are connected by a rotatable -O- group, which allows the ligand with subtle conformational adaptation; (2) seven potential coordination sites (six carboxylate O and one ether O) of H_3cpta ligand, which can provide more varied coordination patterns in the construction of fascinating coordination frameworks, especially with high dimensionalities. However, the metal-organic networks constructed from the H_3cpta ligand have not been reported.

Taking into account these factors, we herein report the syntheses, crystal structures, and magnetic properties of two Co (Ⅱ) coordination polymers constructed from H_3cpta.

1 Experimental

1.1 Reagents and physical measurements

All chemicals and solvents were of AR grade and used without further purification. The content of carbon, hydrogen and nitrogen were determined using an Elementar Vario EL elemental analyzer. IR spectra were recorded using KBr pellets and a Bruker EQUINOX 55 spectrometer. Thermogravimetric analysis (TGA) data were collected on a LINSEIS STA PT1600 thermal analyzer with a heating rate of 10 ℃·min^{-1}. Powder X-ray diffraction patterns (PXRD) were determined with a Rigaku-Dmax 2400 diffractometer using Cu $K\alpha$ radiation (λ =0.154 060 nm) and 2θ ranging from 5° to 45°, in which the X-ray tube was operated at 40 kV and 40 mA. Magnetic susceptibility data were collected in the 2~300 K temperature range with a Quantum Design SQUID Magnetometer MPMS XL-7 with a field of 0.1 T. A correction was made for the diamagnetic contribution prior to data analysis.

1.2 Synthesis of $[Co(\mu_2\text{-Hcpta})(phen)(H_2O)]_n$ (1)

A mixture of $CoCl_2\cdot 6H_2O$ (0.071 g, 0.30 mmol), H_3cpta (0.060 g, 0.2 mmol), phen (0.060 g, 0.3 mmol), NaOH (0.016 g, 0.40 mmol), and H_2O (10 mL) was stirred at room temperature for 15 min, and then sealed in a 25 mL Teflon-lined stainless steel vessel, and heated at 160 ℃ for 3 days, followed by cooling to room temperature at a rate of 10 ℃·h^{-1}. Orange block-shaped crystals of **1** were isolated manually, and washed with distilled water. Yield: 63 % (based on H_3cpta). Anal. Calcd. for $C_{27}H_{18}CoN_2O_8$ (%): C 58.18, H 3.26, N 5.03; Found (%): C 58.46, H 3.24, N 5.01. IR (KBr, cm^{-1}): 3 438w, 3 050w, 1 702w, 1 625m, 1 594s, 1 559s, 1 528w, 1 493w, 1 452w, 1 400s, 1 355s, 1 299w, 1 243w, 1 151w, 1 100w, 1 048w, 956w, 850m, 809w, 787w, 762w, 727m, 691w, 665w, 640w, 594w, 537w.

1.3 Synthesis of $[Co_3(\mu_5\text{-cpta})_2(2,2'\text{-bipy})_2]_n$ (2)

The preparation of **2** was similar to that of **1** except 2,2′-bipy (0.047 g, 0.30 mmol) was used instead of phen and different amount of NaOH (0.024 g, 0.60 mmol) was used. Pink block-shaped crystals of **2** were isolated manually, washed with distilled water. Yield: 55% (based on H_3cpta). Anal. Calcd. for $C_{50}H_{30}Co_3N_4O_{14}$: C 55.22, H 2.78, N 5.15; Found(%): C 55.02, H 2.81, N 5.11. IR (KBr, cm^{-1}): 1 590s, 1 554m, 1 529w, 1 477w, 1 452m, 1 396s, 1 345s, 1 237m, 1 156w, 1 094w, 1 059w, 1 018w, 956w, 879w, 870w, 834w, 798m, 767s, 737w, 706w, 661w, 589w, 537m. The compounds are insoluble in water and common organic

solvents, such as methanol, ethanol, acetone and DMF.

1.4 Structure determinations

The data of two single crystals with dimensions of 0.26 mm×0.24 mm×0.21 mm for **1** and 0.27 mm×0.22 mm×0.21 mm for 2, respectively, were collected at 293(2) K on a Bruker SMART APEX Ⅱ CCD diffractometer with Mo $K\alpha$ radiation (λ=0.071 073 nm). The structures were solved by direct methods and refined by full matrix least-square on F^2 using the SHELXTL-97 program[21]. All non-hydrogen atoms were refined anisotropically. All the hydrogen atoms were positioned geometrically and refined using a riding model. A summary of the crystallography data and structure refinements for **1** and **2** is given in Table 1. The selected bond lengths and angles for compounds **1** and **2** are listed in Table 2. Hydrogen bond parameters of compound **1** are given in Table 3.

CCDC: 1507502, **1**; 1507503, **2**.

Table 1 Crystal data for compounds 1 and 2

Compound	**1**	**2**
Chemical formula	$C_{27}H_{18}CoN_2O_8$	$C_{50}H_{30}Co_3N_4O_{14}$
Molecular weight	557.36	1 087.57
Crystal system	Monoclinic	Monoclinic
Space group	$P2_1/c$	$P2_1/c$
a / nm	1.043 61(5)	1.199 75(6)
b / nm	0.792 95(4)	1.494 46(4)
c / nm	2.789 04(14)	1.306 61(7)
β / (°)	94.042(5)	115.402(6)
V / nm^3	2.302 3(2)	2.116 2 (2)
Z	4	2
F(000)	1 140	1 102
θ range for data collection / (°)	3.28~25.05	3.34~25.04
Limiting indices	$-11\leqslant h\leqslant 12$, $-9\leqslant k\leqslant 9$, $-19\leqslant l\leqslant 33$	$-12\leqslant h\leqslant 14$, $-17\leqslant k\leqslant 17$, $-15\leqslant l\leqslant 10$
Reflections collected, unique (R_{int})	8 222, 4 088 (0.056 3)	7 382, 3 733 (0.041 3)
D_c / (g·cm^{-3})	1.608	1.707
μ / mm^{-1}	0.805	1.243
Data, restraints, parameters	4 088, 0, 345	3 733, 0, 322
Goodness-of-fit on F^2	1.080	1.038
Final R indices[$I\geqslant 2\sigma(I)$] R_1, wR_2	0.050 1, 0.070 9	0.043 7, 0.073 9
R indices (all data) R_1, wR_2	0.088 1, 0.086 2	0.064 4, 0.083 0
Largest diff. peak and hole / (e·nm^{-3})	460 and −435	327 and −319

Table 2 Selected bond distances (nm) and bond angles (°) for compounds 1 and 2

1					
Co(1)-O(1)	0.212 7(3)	Co(1)-O(2)A	0.210 1(2)	Co(1)-O(6)A	0.209 3(2)
Co(1)-O(8)	0.203 8(2)	Co(1)-N(1)	0.218 7(3)	Co(1)-N(2)	0.214 8(3)
O(8)-Co(1)-O(6)A	89.09(10)	O(8)-Co(1)-O(2)A	175.40(10)	O(6)A-Co(1)-O(2)A	87.40(10)
O(8)-Co(1)-O(1)	93.85(10)	O(6)A-Co(1)-O(1)	95.90(9)	O(2)A-Co(1)-O(1)	83.56(10)
O(8)-Co(1)-N(2)	93.05(11)	O(6)A1-Co(1)-N(2)	169.13(11)	O(2)A-Co(1)-N(2)	90.95(10)
O(1)-Co(1)-N(2)	94.59(11)	O(8)-Co(1)-N(1)	84.85(11)	O(6)A-Co(1)-N(1)	92.39(11)
O(2)A-Co(1)-N(1)	98.26(11)	O(1)-Co(1)-N(1)	171.59(10)	N(2)-Co(1)-N(1)	77.21(12)

Continued Table 2

			2		
Co(1)-O(1)	0.223 9(2)	Co(1)-O(2)	0.210 9(2)	Co(1)-O(4)B	0.210 6(2)
Co(1)-O(7)A	0.201 7(2)	Co(1)-N(1)	0.214 5(3)	Co(1)-N(2)	0.210 6(3)
Co(2)-O(1)	0.215 0(2)	Co(2)-O(1)B	0.215 0(2)	Co(2)-O(4)	0.213 0(2)
Co(2)-O(4)B	0.213 0(2)	Co(2)-O(6)A	0.209 4(2)	Co(2)-O(6)C	0.209 4(2)
O(7)A-Co(1)-N(2)	91.74(10)	O(7)A-Co(1)-O(4)B	88.19(9)	N(2)-Co(1)-O(4)B	113.48(10)
O(7)A-Co(1)-O(2)	154.32(11)	N(2)-Co(1)-O(2)	109.33(10)	O(4)B-Co(1)-O(2)	96.27(9)
O(7)A-Co(1)-N(1)	80.95(10)	N(2)-Co(1)-N(1)	76.87(11)	O(4)B-Co(1)-N(1)	165.36(10)
O(2)-Co(1)-N(1)	89.49(10)	O(7)A-Co(1)-O(1)	96.02(9)	N(2)-Co(1)-O(1)	166.52(10)
O(4)B-Co(1)-O(1)	77.86(8)	O(2)-Co(1)-O(1)	60.61(9)	N(1)-Co(1)-O(1)	93.45(10)
O(6)A-Co(2)-O(4)	92.21(8)	O(6)C-Co(2)-O(4)	87.79(8)	O(6)A-Co(2)-O(1)	91.99(8)
O(6)C-Co(2)-O(1)	88.01(8)	O(4)-Co(2)-O(1)	100.67(8)	O(4)B-Co(2)-O(1)	79.33(8)
Co(2)-O(1)-Co(1)	94.45(9)	Co(1)B-O(4)-Co(2)	99.06(9)		

Symmetry transformations used to generate equivalent atoms: A: $-x+1$, $y-1/2$, $-z+1/2$ for **1**; A: x, $-y+1/2$, $z-1/2$; B: $-x+1$, $-y+1$, $-z+1$; C: $-x+1$, $y+1/2$, $-z+3/2$ for **2**

Table 3 Hydrogen bond lengths (nm) and angles (°) of compound 1

D-H···A	*d*(D-H) / nm	*d*(H···A) / nm	*d*(D···A) / nm	∠DHA / (°)
O(4)-H(4)···O(7)A	0.082	0.184	0.264 3	164.2
O(8)-H(1W)···O(1)B	0.082	0.204	0.277 2	148.3
O(8)-H(2W)···O(7)C	0.086	0.198	0.275 9	151.9

Symmetry code: A: $-x+1$, $-y+1$, $-z$; B: $-x+1$, $y+1/2$, $-z+1/2$; C: $-x+1$, $y-1/2$, $-z+1/2$

2 Results and discussion

2.1 Description of the structure

2.1.1 $[Co(\mu_2\text{-Hcpta})(phen)(H_2O)]_n$ (**1**)

The X-ray crystallography analyses reveal that compound **1** has a 1D chain structure. Its asymmetric unit contains one crystallographically unique Co(Ⅱ) atom, one μ_2-$Hcpta^{2-}$ block, one phen moiety, and one coordination water molecule. As depicted in Fig.1, the six-coordinated Co1 atom displays a distorted octahedral $\{CoN_2O_4\}$ geometry filled by four O atoms from two different μ_2-$Hcpta^{2-}$ blocks and one coordinated water molecule and two N atoms from one phen ligand. The lengths of the Co-O bonds range from 0.203 8(2) to 0.212 7(3) nm, whereas the Co-N distances vary from 0.214 8(3) to 0.218 7(3) nm; these bonding parameters are comparable to those found in other reported Co(Ⅱ) compounds[10,22-24]. In **1**, the $Hcpta^{2-}$ ligand acts as a μ_2-linker (Scheme 1, mode Ⅰ), in which two deprotonated carboxylate groups show the

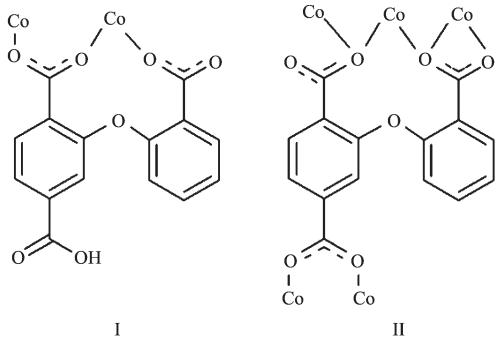

I II

Scheme 1 Coordination modes of $Hcpta^{2-}$/$cpta^{3-}$ ligands in compounds **1** and **2**

$\eta^1:\eta^0$ monodentate and $\eta^1:\eta^1$ bidentate modes, respectively. The dihedral angle between two phenyl rings in the $Hcpta^{2-}$ is 81.03°. The angle of C-$O_{etheric}$-C is 119.16°. The carboxylate groups of $Hcpta^{2-}$ ligands bridge alternately neighboring Co(Ⅱ) atoms in a *syn-anti* coordination fashion to form a 1D chain with the Co⋯Co separation of 0.505 5(3) nm (Fig.2). The present structure shows 1D zigzag metal organic chain wherein the 2-connected Co1 nodes are interconnected by the μ_2-$Hcpta^{2-}$ linkers (Fig.3). These chains can be

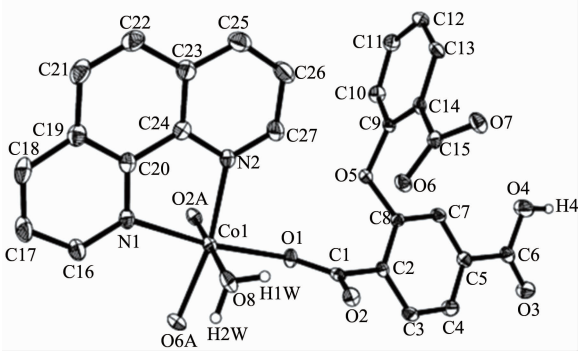

Hydrogen atoms were omitted for clarity except those of COOH groups; Symmetry codes: A: −*x*+1, *y*−1/2, −*z*+1/2

Fig.1　Drawing of the asymmetric unit of compound **1** with 30% probability thermal ellipsoids

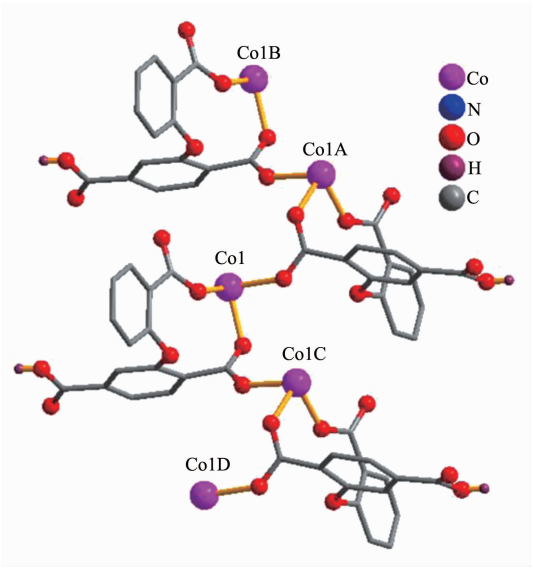

Phen ligands are omitted for clarity; Symmetry codes: A: −*x*+1, *y*+1/2, −*z*+1/2; B: *x*, *y*+1, *z*; C: −*x*+1, −1/2+*y*, −*z*+1/2; D: *x*, *y*−1, *z*

Fig.2　View of a 1D metal-organic chain parallel to the *bc* plane

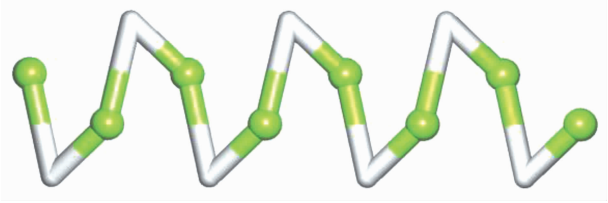

Viewed along the a axis; Color codes: 2-connected Co1 nodes (greenish yellow balls), centroids of 2-connected μ_2-$Hcpta^{2-}$ linkers (gray)

Fig.3　Topological representation of a 1D metal-organic zigzag chain in **1** displaying a uninodal 2-connected underlying net with the 2C1 topology

topologically classified as a uninodal 2-connected net with the 2C1 topology. The adjacent chains are connected together by O-H···O hydrogen bonds (Table 3), forming a 2D supramolecular sheet (Fig.4).

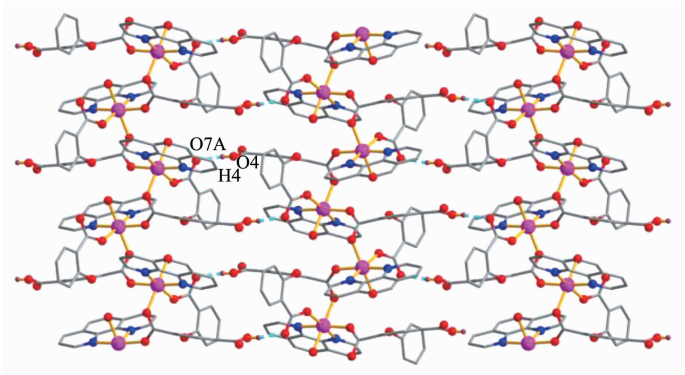

Blue lines present the H-bonds; Symmetry codes: A: $-x+1$, $-y+1$, $-z$

Fig.4 Perspective of a 2D supramolecular network along the *bc* plane in **1**

2.1.2 $[Co_3(\mu_5\text{-cpta})_2(2,2'\text{-bipy})_2]_n$ (**2**)

The asymmetric unit of **2** consists of two crystallographically distinct Co(Ⅱ) atoms (Co1 with full occupancy; Co2 is located on a 2-fold rotation axis), one μ_5-cpta^{3-} block, and one 2,2′-bipy ligand. As shown in Fig.5, the Co1 atom is six-coordinated and adopts a distorted octahedral $\{CoN_2O_4\}$ geometry completed by four carboxylate O from three distinct μ_5-cpta^{3-} blocks and two N atoms from one 2,2′-bipy ligand. The six-coordinated Co2 center is located on a 2-fold rotation axis and is surrounded by six O atoms from six different cpta^{3-} blocks, thus adopting a distorted octahedral $\{CoO_6\}$ geometry. The Co-O distances range from 0.201 7(2) to 0.223 9(2) nm, whereas the Co-N distances vary from 0.210 6(3) to 0.214 5(3) nm; these bonding parameters are comparable to those observed in other Co(Ⅱ) compounds[10,22-24]. In **2**, the cpta^{3-} block acts as a μ_5-spacer (Scheme 1, mode Ⅱ), in which the carboxylate groups exhibit the μ_2-η^1:η^1 and μ_2-η^0:η^2 bidentate and μ_2-η^1:η^2 tridentate modes. In the cpta^{3-}, the dihedral angle between the two phenyl rings is 87.37°. The angle C-O$_{etheric}$-C is 119.73°. Three adjacent Co(Ⅱ) ions are bridged by means of six carboxylate groups from the four different cpta^{3-} blocks, giving rise to a centrosymmetric tricobalt(Ⅱ) subunit (Fig.6). In this Co_3 unit, the Co···

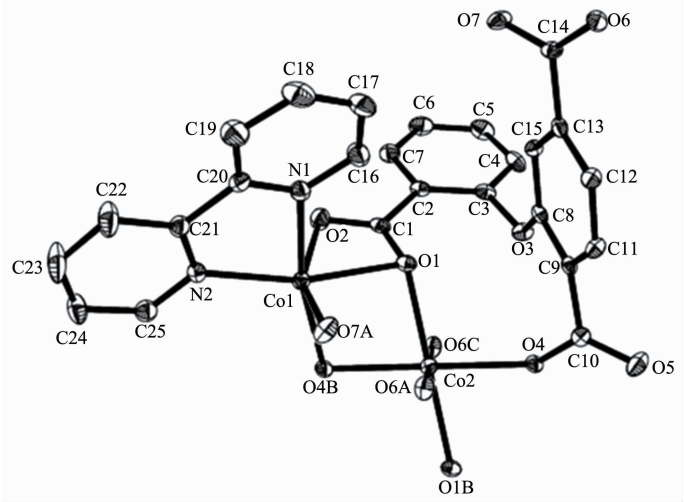

Hydrogen atoms were omitted for clarity, Symmetry codes: A: x, $-y+1/2$, $z-1/2$; B: $-x+1$, $-y+1$, $-z+1$; C: $-x+1$, $y+1/2$, $-z+3/2$

Fig.5 Drawing of the asymmetric unit of compound 2 with 30% probability thermal ellipsoids

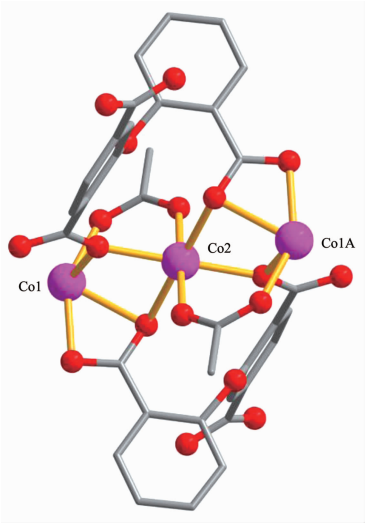

Symmetry code: A: $-x+1, -y+1, -z+2$

Fig.6 Tricobalt(Ⅱ) subunit in compound **2**

Co distance of 0.322 3(3) nm is close to those reported for other carboxylate-bridged trinuclear Co(Ⅱ) compounds[25-27]. The adjacent Co_3 subunits are further interlinked by the $cpta^{3-}$ blocks into a 2D metal-organic network (Fig.7). It has the shortest distance of 1.107 0(3) nm between the neighboring tricobalt(Ⅱ)

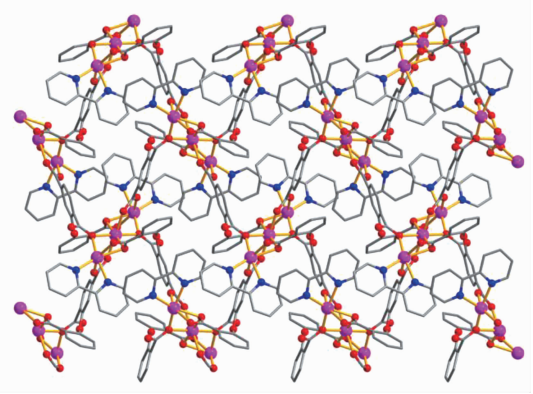

Fig.7 2D metal-organic framework along the *a* axis in compound **2**

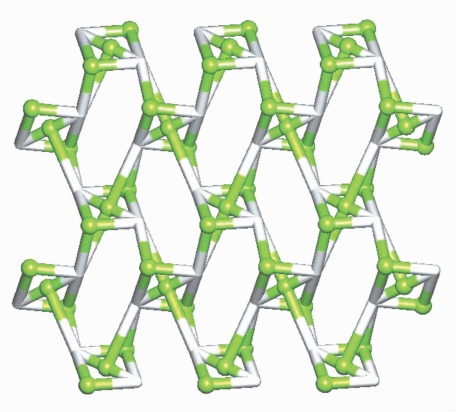

Viewed along the *a* axis; Color codes: 3-connected Co1 and 4-connected Co2 nodes (greenish yellow balls), centroids of 5-connected μ_5-$cpta^{3-}$ nodes (gray)

Fig.8 Topological representation of a 2D metal-organic network in **2** displaying a trinodal 3,4,5-connected underlying layer with the 3,4,5L45 topology and point symbol of $(4^3)_2(4^4.8^6)_2(4^5.6)$

subunits. This structure features an intricate 2D metal-organic layer, which from the topological point of view, is assembled from the 3-connected Co1 and 4-connected Co2 nodes, as well as the 5-connected μ_5-cpta^{3-} nodes (Fig.8). Its topological analysis discloses a trinodal 3,4,5-connected underlying net with a very rare 3,4,5L45 topology and point symbol of $(4^3)_2(4^4.8^6)_2(4^5.6)$. The (4^3), $(4^4.8^6)$, and $(4^5.6)$ notations correspond to the Co1, μ_5-cpta^{3-}, and Co2 nodes, respectively.

2.2 TGA analysis and PXRD results

To determine the thermal stability of compounds **1** and **2**, their thermal behaviors were investigated under nitrogen atmosphere by thermogravimetric analysis (TGA). As shown in Fig.9, the TGA curve of **1** reveals that one coordinated aqua ligand is released between 148~210 ℃ (Obsd. 3.5%; Calcd. 3.2%), and the dehydrated solid begins to decompose at 308 ℃. The TGA curve of **2** indicates that the compound is stable up to 367 ℃, and then decompose upon further heating. The patterns for the as-synthesized bulk material closely match the simulated ones from the single-crystal structure analysis, which is indicative of the pure solid-state phase (Fig.10 and 11).

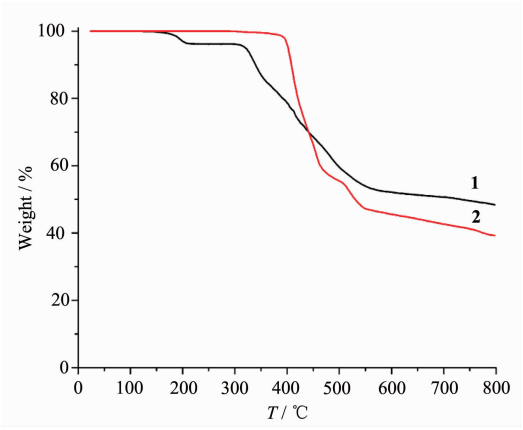

Fig.9 TGA curves of compounds **1** and **2**

2.3 Magnetic properties

Variable-temperature magnetic susceptibility studies were carried out on powder samples of compounds **1** and **2** in the 2 ~300 K temperature range. For **1**, as shown in Fig.12, the room temperature values of $\chi_M T$(3.21 cm^3·mol^{-1}·K) is larger than the value (1.83 cm^3·mol^{-1}·K) expected for one magnetically isolated high-spin Co(Ⅱ) ions (S=3/2, g= 2.0). This is a common phenomenon for Co(Ⅱ) ions due to their strong spin-orbital coupling interactions[10,22-24]. When the temperature is lowered, the $\chi_M T$ values decrease slowly until about 116 K, then decrease quickly to 1.23 cm^3·mol^{-1}·K at 2.0 K. Between 88

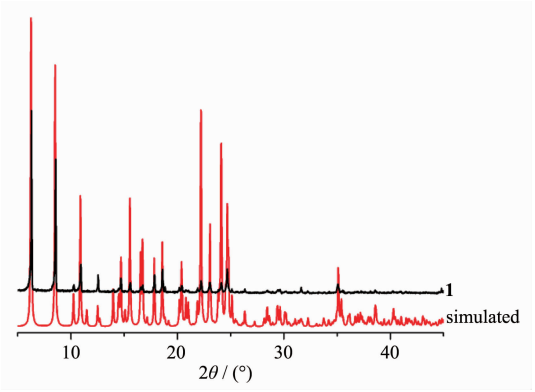

Fig.10 PXRD patterns of compound **1** at room temperature

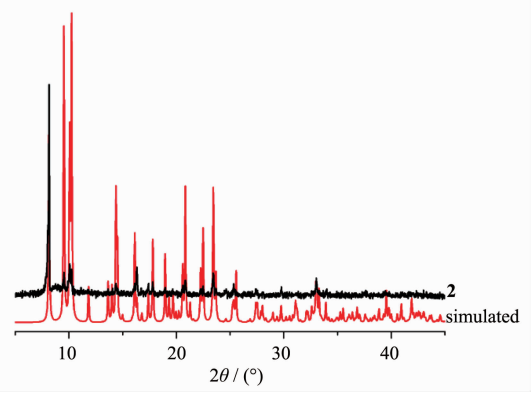

Fig.11 PXRD patterns of compound **2** at room temperature

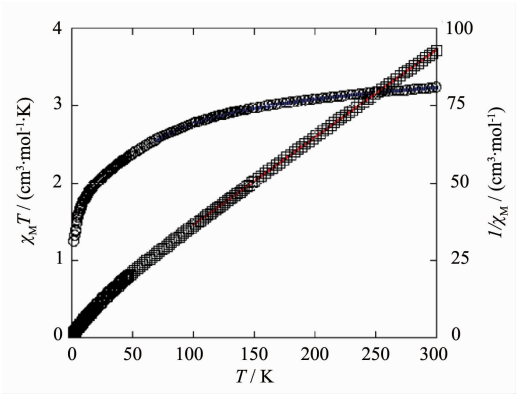

The blue curve represents the best fit to the equations in the text; The red line shows the Curie-Weiss fitting

Fig.12 Temperature dependence of $\chi_M T$ (O) and $1/\chi_M$(□) vs T for compound **1**

and 300 K, the magnetic susceptibilities can be fitted to the Curie-Weiss law with C=3.55 cm^3·mol^{-1}·K and θ=−28.4 K. These results indicate an antiferromagnetic interaction between the adjacent Co (Ⅱ) centers in compound **1**. We tried to fit the magnetic data of **1** using the following expression for a 1D Co(Ⅱ) chain[28]:

$$\chi_{chain} = [Ng^2\beta^2/(kT)][2.0+0.019\ 4x+0.777x^2][3.0+4.346x+3.232x^2+5.834x^3]^{-1}$$

$$x = |J|/(kT)$$

Using this rough model, the susceptibilities above 65 K were simulated, leading to J=−9.87 cm^{-1}, g=2.43. The negative J parameters indicate that an weak antiferromagnetic exchange coupling exists between the adjacent Co(Ⅱ) centers in **1**, which is agreement with negative θ value. According to the structure of **1**, there is one magnetic exchange pathway within the chain through one syn-anti carboxylate bridges, which could be responsible for the observed antiferromagnetic exchange.

For the cobalt(Ⅱ) network **2**, as shown in Fig.13, the $\chi_M T$ value at room temperature of 8.85 cm^3·mol^{-1}·K, is much larger than the value (5.61 cm^3·mol^{-1}·K) expected for three magnetically isolated high-spin Co (Ⅱ) ions with S=3/2. Upon lowering the temperature, the $\chi_M T$ value rapidly decreases to a minimum value of 7.96 cm^3·mol^{-1}·K at 21 K, then abruptly increases to a sharp maximum (9.59 cm^3·mol^{-1}·K) at 2.9 K. Finally, it decreases to 9.27 cm^3·mol^{-1}·K at 2 K. In the 50~300 K range, the magnetic susceptibilities can be fitted to the Curie-Weiss law with C=9.06 cm^3·mol^{-1}·K and θ=−8.9 K. It should be noted that magnetic research for high spin Co system is fairly complicated and difficult because many factors, especially the strong spin-orbital coupling, can influence the magnetic behavior. The first decrease for $\chi_M T$ value (300~21 K) and the small negative θ value may be mainly due to the strong spin-orbital coupling of the single-ion behavior at high temperature. The $\chi_M T$ value abruptly increases (21~2.9 K) can be interpreted by ferromagnetic coupling interactions within the Co_3 unit, which is strong enough to compensate for the single-ion behavior resulting from spin-orbital coupling. The magnetic data can be fit by an expression for the S=3/2 system with dominant zero field splitting effects, D, and the magnetic coupling (zJ) between the neighboring Co(Ⅱ) centers, neglecting the magnetic coupling between the two terminal Co(Ⅱ) centers within the Co_3 unit[25-27]:

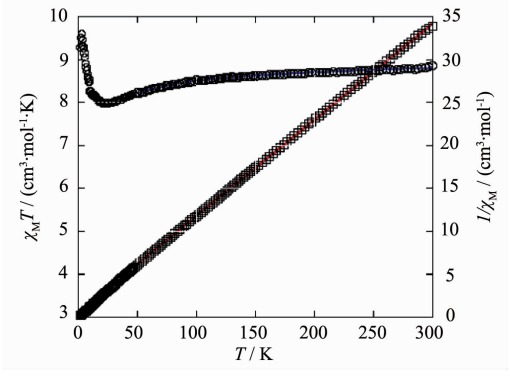

The blue curve represents the best fit to the equations in the text; The red line shows the Curie-Weiss fitting

Fig.13 Temperature dependence of $\chi_M T$ (O) and $1/\chi_M$(□) vs T for compound **2**

$$\chi_{//} = \frac{Ng^2\mu_B^2}{kT}\frac{1+9e^{-2D/(kT)}}{4[1+e^{-2D/(kT)}]}$$

$$\chi_{\perp} = \frac{Ng^2\mu_B^2}{kT}\frac{4+(3kT/D)[1+e^{-2D/(kT)}]}{4[1+e^{-2D/(kT)}]}$$

$$\chi' = \frac{\chi_{//}+2\chi_{\perp}}{3}$$

$$\chi = \frac{\chi'}{1-\frac{2zJ}{Ng^2\mu_B^2}\chi'}$$

Where N is Avogadro's number, μ_B is Bohr magneton, k is Boltzmann's constant, and g is Lande factor. The best fit in the range of 50~300 K was obtained with values of g=2.37, D=96.3 cm^{-1}, and zJ=0.78 cm^{-1} with the agreement factor R ($R=\sum[(\chi_M T)_{obs}-(\chi_M T)_{calc}]^2/\sum(\chi_M T)^2$) of 5.76×10^{-5}. The main magnetic exchange pathway is the exchange between adjacent Co (Ⅱ) ions within the Co_3 cluster to the μ_2-$O_{carboxyl}$ bridge with the superexchange angle Co-$O_{carboxyl}$-Co of 99.05(3)°.

3 Conclusions

In summary, two new coordination polymers, namely $[Co(\mu_2\text{-Hcpta})(phen)(H_2O)]_n$ (**1**) and $[Co_3(\mu_5\text{-cpta})_2(2,2'\text{-bipy})_2]_n$(**2**) have been synthesized under hydrothermal conditions. The compounds feature the 1D chain and 2D sheet structures, respectively.

Magnetic studies for two compounds show an antiferromagnetic coupling between the adjacent Co(Ⅱ) centers.

References:

[1] Sun Y J, Zhou H C. *Sci. Technol. Adv. Mater.*, **2015**,**16**: 054202

[2] Li J R, Sculley J, Zhou H C. *Chem. Rev.*, **2012**,**112**:869-932

[3] Cui Y, Yue Y, Qian G, et al. *Chem. Rev.*, **2012**,**112**:1126-1162

[4] Kuppler R J, Timmons D J, Fang Q R, et al. *Coord. Chem. Rev.*, **2009**,**253**:3042-3066

[5] Zheng X D, Lu T B. *CrystEngComm*, **2010**,**12**:324-336

[6] Jiang X, Liu C M, Kou H Z. *Inorg. Chem.*, **2016**,**55**:5880-5885

[7] Zhang W J, Yuan D Q, Liu D H, et al. *Chem. Mater.*, **2012**, **24**:18-25

[8] Zhang H, Yang J, Liu Y Y, et al. *Cryst. Growth Des.*, **2016**, **16**:3244-3255

[9] Karmakar A, Desai A V, Ghosh S K, *Coord. Chem. Rev.*, **2016**,**07**:313-341

[10]Gu J Z, Gao Z Q, Tang Y. *Cryst. Growth Des.*, **2012**,**12**: 3312-3323

[11]Gao Q, Xie Y B, Li J R, et al. *Cryst. Growth Des.*, **2012**,**12**: 281-288

[12]Lee J, Kang Y J, Cho N S, et al. *Cryst. Growth Des.*, **2016**,**16**:996-1004

[13]Li L, Cao X Y, Huang R D. *Chin. J. Chem.*, **2016**,**34**:143-156

[14]Lu W G, Su C Y, Lu T B, et al. *J. Am. Chem. Soc.*, **2006**, **128**:34-35

[15]Wang H H, Yang H Y, Shu C H, et al. *Cryst. Growth Des.*, **2016**,**16**:5394-5402

[16]Cui L T, Niu Y F, Han J, et al. *J. Solid State Chem.*, **2015**,**227**:155-164

[17]Wang H L, Zhang D P, Sun D F, et al. *CrystEngComm*, **2010**,**12**:1096-1102

[18]Chen X, Wang Y Y, Liu B, et al. *Dalton Trans.*, **2013**,**42**: 7092-7100

[19]Hu J S, Huang X H, Pan C L, et al. *Cryst. Growth Des.*, **2015**,**15**:2272-2281

[20]Zhao H W, Li B. *Chin. J. Struct. Chem.*, **2012**,**31**:61-66

[21]Sheldrick G M. *SHELXTL*-97, University of Göttingen, Germany, **1997**.

[22]Tang L, Fu F, Wang J J, et al. *Polyhedron*, **2015**,**88**:116-124

[23]GU Jin-Zhong(顾金忠), GAO Zhu-Qing(高竹青), DOU Wei(窦伟), et al. *Chinese J. Inorg. Chem.*(无机化学学报), **2009**,**25**(5):920-923

[24]QIAO Yu(乔宇), WEI Bing(尉兵), WANG Lu-Yao(王璐瑶), et al. *Chinese J. Inorg. Chem.*(无机化学学报), **2016**,**32**(7): 1261-1266

[25]Marshall S R, Rheingold A L, Dawe L N, et al. *Inorg. Chem.*, **2002**,**41**:3599-3601

[26]Su Z, Fan J, Chen M, et al. *Cryst. Growth Des.*, **2011**,**11**: 1159-1169

[27]Niu C Y, Zheng X F, Wan X S, et al. *Cryst. Growth Des.*, **2011**,**11**:2874-2888

[28]Kahn O. *Molecular Magnetism*. New York: VCH Publishers, **1993**:258